To cite this article: CUI H W, DING Q Y. Analysis of ultimate load-bearing behavior of stiffened plate under axial cyclic loading[J/OL]. Chinese Journal of Ship Research, 2022, 17(4). http://www.ship-research.com/en/article/doi/10.19693/j.issn.1673-3185.02400.

DOI: 10.19693/j.issn.1673-3185.02400

Analysis of ultimate load-bearing behavior of stiffened plate under axial cyclic loading

CUI Huwei, DING Qiyin*

School of Shipping and Naval Architecture, Chongqing Jiaotong University, Chongqing 400074, China

Abstract: [**Objectives**] In order to improve the accuracy of nonlinear numerical simulation of the ultimate load-bearing behavior of the stiffened plates of a hull, the effects of ideal elastoplastic, isotropic hardening, and cyclic plastic Chaboche material models on the plastic yield distribution, compression, and tensile ultimate strength of stiffened plates in their ultimate state are studied. **[Methods]** For a stiffened plate of the same size, software ANSYS is used to carry out non-linear finite element numerical simulation of ultimate bearing performance under axial cyclic compression and cyclic compression-tension loads. [**Results**] The results show that different material properties have a significant impact on the ultimate bearing capacity of stiffened plates and the plastic yield distribution in the ultimate state. When carrying out the nonlinear finite element numerical simulation of the ultimate bearing behavior of the stiffened plate of a hull, we should select the appropriate material model according to different load forms. [**Conclusions**] The results of this study can provide valuable references for further research on the ultimate strength characteristics and cumulative plastic failure mechanisms of hull structures under cyclic loading.

Key words: cyclic loading; stiffened plate; cyclic plasticity; ultimate strength

CLC number: U661.3

0 Introduction

The total longitudinal strength of hull girders is the most important guarantee for the safety of hulls. With the gradual application of the concept of ultimate strength in the structural design of ships, hull design requires not only determination of hull size but also accurate evaluation of the ultimate strength of hulls. For a long time, the ultimate strength of hulls has mainly been evaluated on the basis of static ultimate strength of one-time failure. Caldwell evaluated the ultimate strength of hull girders for the first time and published a paper on the calculation of the ultimate strength of hull girders in 1965[1]. This indicates that the concept of static ultimate strength evaluation of hull girders entered a substantive stage of objective research. At present, research based on this concept is mature and has entered a practical stage. Since April 2006, ultimate strength evaluation of oil tankers and bulk carriers has been incorporated into mandatory requirements of common structural rules [2-3] by the International Association of Classification Societies (IACS). Afterward, International Standardization Organization (ISO) [4] and International Maritime Organization (IMO) [5-6] have successively incorporated ultimate strength evaluation provisions of hull girders into their regulations. All the above evaluation provi-

Received: 2021 – 06 – 03 **Accepted:** 2021 – 09 – 21

Supported by: The National Natural Science Foundation for Young Scientists of China (52001040); Science and Technology Research Project of Chongqing Municipal Education Commission (KJQN202000712); The General Program of Natural Science Foundation of Chongqing (cstc2021jcyj-msxmX0944); Open Fund of National Engineering Research Center for Water Transport Safety (A2021003)

Authors: CUI Huwei, male, born in 1986, Ph.D., associate professor. Research interest: ultimate strength evaluation of hulls. E-mail: hwcui@cqjtu.edu.cn

DING Qiyin, male, born in 1998, master degree candidate. Research interest: ultimate strength evaluation of hulls. E-mail: d1501023677@163.com

***Corresponding author:** CUI Huwei

sions are based on static ultimate strength evaluation of onetime failure.

Objectively speaking, with cyclic wave loads, hull girders are subjected to cyclic total longitudinal bending moment and deformation. As static ultimate strength criteria fail to consider the influence of cyclic loading, some scholars believe that the concept of the ultimate strength of cumulative plastic failure or shakedown failure of hulls from the perspective of cyclic loading is more consistent with failure mechanisms of the ultimate strength of hulls. Refs [7] and [8] successively proposed that attention should be paid to hull failure caused by cumulative plasticity under cyclic loading. People are always enlightened through disasters and reflection on failure. For example, the Japanese bulk carrier "Onomichi Maru" encountered heavy wind and waves and suffered severe slamming, which resulted in a breakoff of its hull at a dangerous section. On this basis, many well-known Japanese scholars re-proposed cumulative plastic failure of hulls [9]. In China, Huang et al. [10-12] first emphasized the importance of research on the cumulative plastic failure of hulls under cyclic loading. They believed that cumulative plastic failure criteria were a development direction of static ultimate strength criteria and should be an important aspect in future research on the total strength of ships. In recent years, preliminary achievements have been obtained in research on the ultimate strength of cumulative plastic failure of hulls under cyclic loading. Cui et al. [13-17] studied the ultimate strength of cumulative plastic failure of hulls under cyclic loading. The ultimate strength of shakedown failure of hull girders under cyclic loading was put forward in the same period when Caldwell put forward static ultimate strength[1]. Jones [18] first introduced elastic shakedown of a hull under cyclic loading into the ultimate strength study of a hull girder. According to Jones's research, when the elastic shakedown effect of a hull under cyclic loading is considered, the vertical bending-moment bearing capacity of a hull girder is always lower than or never exceeds the static ultimate strength of one-time failure of the hull girder. On this basis, Jones believed that hull girders should be evaluated on the basis of the ultimate strength of shakedown failure rather than the static ultimate strength of onetime failure proposed by Caldwell [1]. Gannon et al. [19] investigated the influence of the shakedown effect on welding-induced residual stress of T-shaped stiffened hull plates by a nonlinear finite element method (FEM). They found that the potential for higher ultimate strength due to the shakedown effect depended on the failure modes of stiffened plates. Regarding the shakedown failure of a hull girder under cyclic bending moment as an important aspect to evaluate and ensure the total longitudinal strength of a ship, Zhang et al. [20] calculated the critical elastic shakedown bending moment of the hull girder under the cyclic bending moment by an incremental FEM.

The above research on the ultimate strength of cumulative plastic failure and shakedown failure of hulls is conducive to the high-precision evaluation of the ultimate strength of hulls. However, it is not sufficient and requires further exploration. Of all the existing methods for ultimate strength evaluation of hull girders, the most representative ones are the nonlinear FEM and Smith's progressive collapse method [21], and the systematic introductions to the two evaluation methods can be found in Ref. [22]. In the evaluation of the static ultimate strength of hulls based on the nonlinear FEM, the strengthening potential of hull materials is taken as the safety margin of evaluated ultimate strength. In view of this, ideal elastoplastic models are widely used for the constitutive relation of hull materials, namely that the plasticity-strengthening effect of materials is ignored. The basic feature of Smith's method is that a cross-section of a hull girder is divided into a series of ribband-stiffener composed structural units. In this method, the average stress-strain relationship of each unit needs to be preset before the ultimate strength of progressive collapse of a hull girder is calculated. The core is to find a suitable average stress-strain relationship of structural units. A stiffened hull plate is the basic member of a hull girder, and its ultimate load-bearing behavior under axial loading determines the ultimate bending strength of the hull girder as a whole. This paper focuses on the load-bearing behavior of stiffened plates under cyclic loading rather than the traditional evaluation of static ultimate strength. Taking the average stress-strain relationship of stiffened panel units in Smith's method as the analysis object, this paper discusses the influence of material model selection for nonlinear FE analysis of a stiffened plate on its ultimate load-bearing behavior such as ultimate strength and distribution of plastic deformation under different evaluation concepts or loading modes.

1 FE model

1.1 Model size and boundary conditions

A single-bend double-span model is used, and the influence of web beams is considered. Specifically, web beams are not actually built but replaced by degree-of-freedom constraints, and a single span has a length of 1 000 mm. Boundary conditions of stiffened plates in Ref. [23] are adopted for this model. In other words, the displacement of one end in the loading direction is constrained while the other end is loaded, and the displacement of its cross-sectional nodes in the loading direction is coupled. In the FE-based numerical simulation of cyclic loading, displacement control is used to apply forced displacement to the main nodes, and extracted reaction force and displacement of these nodes are converted into average stress-strain curves of the stiffened plate. Tables 1 and 2 list the geometric dimensions and boundary conditions of the stiffened plate, respectively. In Table 2, U indicates displacement; R indicates rotation; x refers to the lengthwise direction of the plate; y refers to the breadthwise direction of the plate; z refers to the height-wise direction of the stiffener. Shell 181 elements in ANSYS are used to discretize the structure, and Fig. 1 illustrates the nonlinear FE model and geometry of the stiffened plate. Table 3 shows the nonlinear FE calculated ultimate strength of stiffened plates with different grid sizes under single compression. To ensure both calculation accuracy and efficiency, this paper adopts an element size of 25 mm × 25mm.

Table 1 Model size of stiffened plates

Parameter		Value
Plate	Web-beam interval a/mm	1 000
	Interval between adjacent longitudinals b/mm	350
	Thickness t/mm	9
Stiffener (T-section)	Web height h_w /mm	200
	Web thickness t_w /mm	6.4
	Face-plate width b_f /mm	140
	Face-plate thickness t_f /mm	8.8

Table 2 Boundary conditions of stiffened plates

Stiffened plate unit	Boundary condition
Long edge of panel	$Uy = Rx = Rz = 0$
Short edge of panel	Fixed end: $Ux = Ry = Rz = 0$ Loading end: $Ry = Rz = 0$
Web beam	Intersection with the plate: $Uz = 0$ Intersection with the stiffener: $Uy = 0$

Table 3 Numerical calculation results of ultimate strength of stiffened plates with different grid sizes

Grid size (length ×width) /mm	Ultimate strength/MPa
50×50	280.98
25×25	277.67
12.5×12.5	276.56

1.2 Initial defects

Due to uneven thermal distribution in welding, hulls may have initial defects after manufacturing. Such defects are mainly composed of two parts: One is welding-induced residual stress of hulls, and the other is welding-induced initial deflection. Considering that welding-induced residual stress can be released to some extent under cyclic loading, this paper only takes initial deflection into account. The initial deflection of the stiffened plate in this paper consists of the following three parts.

1) Initial deflection W_{opl} of the plate:

$$W_{opl} = A_0 \sin\frac{m\pi x}{a}\sin\frac{\pi y}{b} \tag{1}$$

2) Beam column-type initial deflection W_{oc} of the stiffener:

$$W_{oc} = B_0 \sin\frac{\pi x}{a}\sin\frac{\pi y}{B} \tag{2}$$

3) Sideway initial deflection W_{os} of the stiffener:

$$W_{os} = C_0 \frac{z}{h_w}\sin\frac{\pi x}{a} \tag{3}$$

where B is the stiffened-plate breadth; A_0, B_0, and

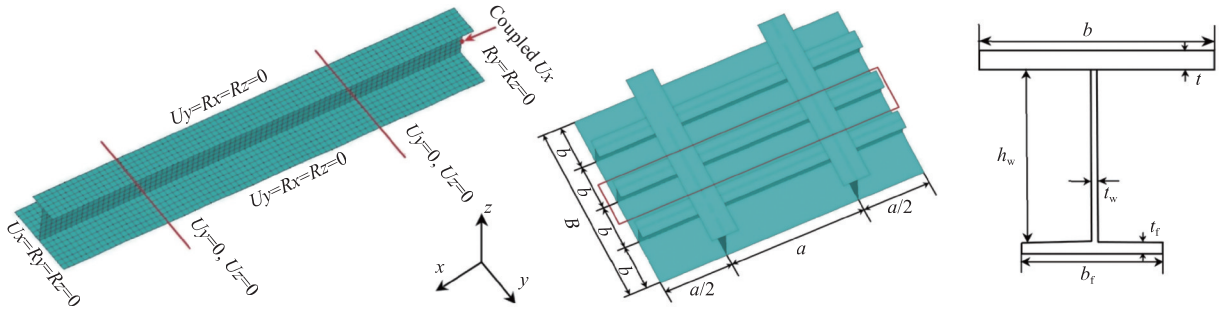

(a) Nonlinear finite-element model of stiffened plate unit (b) Geometry of stiffened plate

Fig. 1 Schematic diagram of stiffened plate unit and stiffened plate structure

C_0 are the amplitude of the three kinds of initial deformation; m is the half-wave number of initial deflection in the x direction. The initial deflection amplitude of an average level is taken as follows: $A_0 = 0.1\beta^2 t$, and $B_0 = C_0 = 0.001\ 5a$, where β is a flexibility coefficient, and $\beta = (b/t)\sqrt{\sigma_Y/E}$; σ_Y is the yield strength, and E is the elastic modulus. In this paper, the initial deflection is applied to the nonlinear FE model by APDL in ANSYS.

2 Constitutive relation of materials and loading conditions

The constitutive relation of steel, namely, steel properties, affects nonlinear FE numerical simulation significantly, and in particular, material strengthening caused by plastic deformation needs to be carefully considered. Under the currently-used conventional concept of static ultimate strength of onetime failure, the ideal elastoplastic constitutive relation is widely used to evaluate the ultimate strength of hulls. Conservative results are obtained as the plasticity-strengthening effect of materials is ignored, and thus, material plasticity strengthening can be regarded as the margin of structural safety. In addition, if structures are under cyclic loading producing large plastic deformation, the plasticity strengthening of materials under cyclic loading should be first determined. In view of different loading cases, this paper uses the ideal elastoplastic constitutive relation, isotropic hardening constitutive relation, and Chaboche constitutive relation of materials considering reverse-loading Bauschinger effect [24] separately. Related parameters of Chaboche constitutive relation of materials can be found in Ref. [25], with an elastic modulus of E = 205 800 MPa, Poisson's ratio of v=0.3, yield strength of σ_Y=285 MPa, and steel grade of S275 [25]. Table 4 lists specific loading conditions and constitutive relations of materials. In the table, ε_Y is the initial yield strain, and G is the shear modulus.

Table 4 Loading mode and material properties

Case No.	Amplitude	Cycle mode	Number of cycles	Material properties	Material parameters
1	$2.5\varepsilon_Y$	Single compression	–	Ideal elastoplasticity	E=207 000 MPa, v=0.3, σ_Y=310.5 MPa, ε_Y = 0.001 5
2	$1.5\varepsilon_Y - 2.0\varepsilon_Y - 2.5\varepsilon_Y$	Cyclic compression	3		
11	$2.5\varepsilon_Y$	Single compression	–	Isotropic hardening	E=207 000 MPa, v=0.3, σ_Y=310.5 MPa, G=10 000 MPa, ε_Y = 0.001 5
22	$1.5\varepsilon_Y - 2.0\varepsilon_Y - 2.5\varepsilon_Y$	Cyclic compression	3		
3	$4.0\varepsilon_Y$	Single compression	–	Ideal elastoplasticity	E=207 000 MPa, v=0.3, σ_Y=310.5 MPa, ε_Y = 0.001 5
4	$2.0\varepsilon_Y - 3.0\varepsilon_Y - 4.0\varepsilon_Y$	Cyclic compression	3		
33	$4.0\varepsilon_Y$	Single compression	–	Isotropic hardening	E=207 000 MPa, v=0.3, σ_Y=310.5 MPa, G=10 000 MPa, ε_Y = 0.001 5
44	$2.0\varepsilon_Y - 3.0\varepsilon_Y - 4.0\varepsilon_Y$	Cyclic compression	3		
5	$\pm1.5\varepsilon_Y$	Cyclic compression-tension	3	Ideal elastoplasticity	E=205 800 MPa, v=0.3, σ_Y=285 MPa, ε_Y = 0.001 38
6	$\pm1.8\varepsilon_Y$				
7	$\pm2.0\varepsilon_Y$				
55	$\pm1.5\varepsilon_Y$		3	Cyclic plasticity	Chaboche model, ε_Y = 0.001 38
66	$\pm1.8\varepsilon_Y$				
77	$\pm2.0\varepsilon_Y$				
8	$\pm1.8\varepsilon_Y$	Cyclic compression-tension	10	Ideal elastoplasticity	E=205 800 MPa, v=0.3, σ_Y=285 MPa, ε_Y = 0.001 38
88	$\pm1.8\varepsilon_Y$			Cyclic plasticity	Chaboche model, ε_Y = 0.001 38

3 Calculation results

In order to observe the plastic yield distribution of the stiffened plate in each cyclic compressive limit state, this paper presents the contours of von Mises stress of the plate in the limit state of each cycle. Generally, an average stress-strain curve can be used to reflect the load-bearing behavior of an entire structure, in which the average stress can be obtained by dividing the reaction force of main nodes by cross-sectional areas. In an average stress-strain curve, the maximum average stress of a stiffened plate under compression reflects the ultimate compressive strength of the stiffened plate. The average

stress-strain curve of the stiffened plate under cyclic loading is given below.

3.1 Von Mises stress distribution in limit state of stiffened plate under cyclic compressive loading

Figs. 2-4 illustrate distributions of von Mises stress in each limit state of the stiffened plate using ideal elastoplastic and isotropic hardening material models separately under maximum cyclic compressive amplitude of $2.0\varepsilon_Y$, in Cases 4 and 44. The red zones in these figures represent plastic yield zones. With the increase in the compressive amplitude of each cycle, in Case 4, the yield zone of the ribband changes from a uniform distribution to central concentration, and plasticity accumulation distinctly occurs in the collapse zone in the middle of the ribband. In Case 44, the yield zone tends to expand, and plasticity accumulation occurs in the whole range of the stiffened plate. The isotropic hardening material model greatly affects the plastic yield zone of the stiffened plate in the first compressive limit state. However, its influence gradually declines in the subsequent cycles. Fig. 4 shows that the yield zone distribution in the third compressive limit state is consistent in Cases 4 and 44.

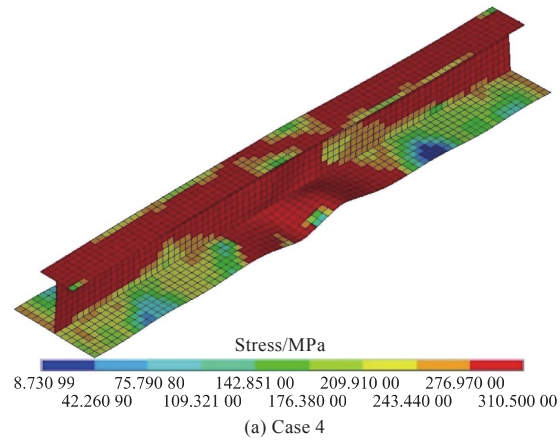

(a) Case 4

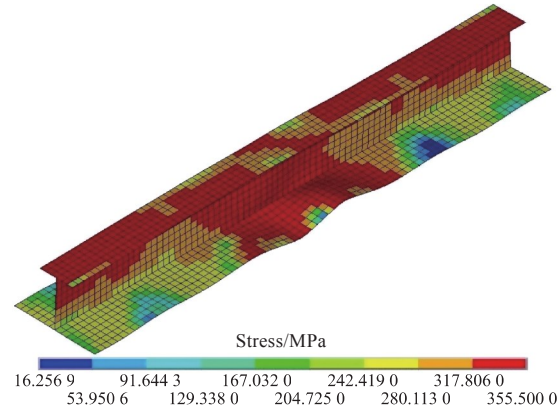

(b) Case 44

Fig. 3 Second compressive limit state of Case 4 and Case 44

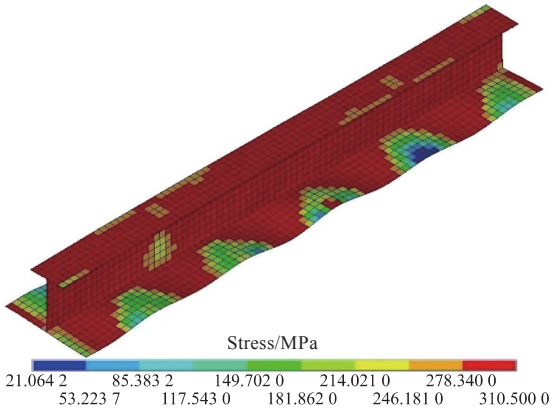

(a) Case 4

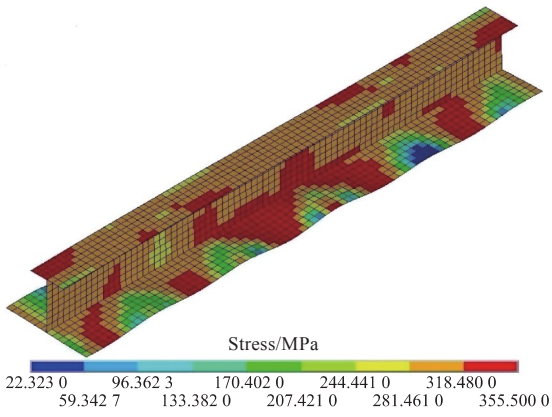

(b) Case 44

Fig. 2 First compressive limit state of Case 4 and Case 44

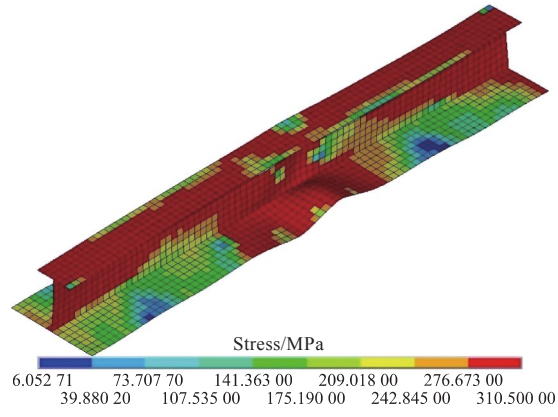

(a) Case 4

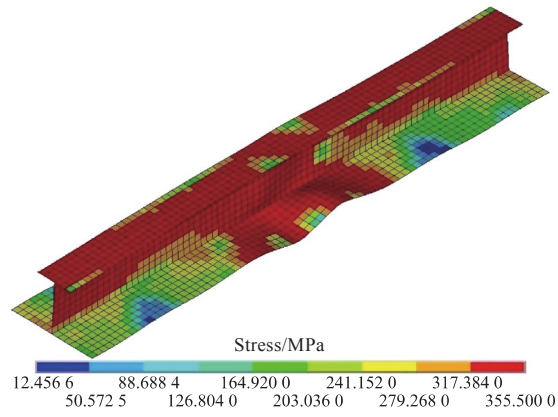

(b) Case 44

Fig. 4 Third compressive limit state of Case 4 and Case 44

3.2 Average stress-strain curves of stiffened plate under cyclic compressive loading

Fig. 5 shows average stress-strain curves under single and cyclic compression in the case of ideal elastoplastic and isotropic hardening material models. In the figure, σ/σ_Y is the average stress, and $\varepsilon/\varepsilon_Y$ is the average strain. It can be found that the ultimate compressive strength of the isotropic hardening material model is always higher than that of the ideal elastoplastic one. The ultimate compressive strength of each cycle of the two material models drops with the increase in strain, and the reloading path in a cycle roughly coincides with the unloading one in the previous cycle. For the ideal elastoplastic material model, curves under single compression can be approximately used as envelopes of curves under cyclic loading. For the isotropic hardening material model, curves under single compression are slightly lower than the envelope of curves under cyclic loading.

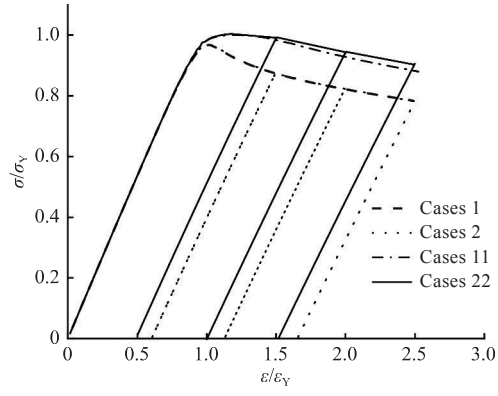

(a) Cases 1,2,11 and 22

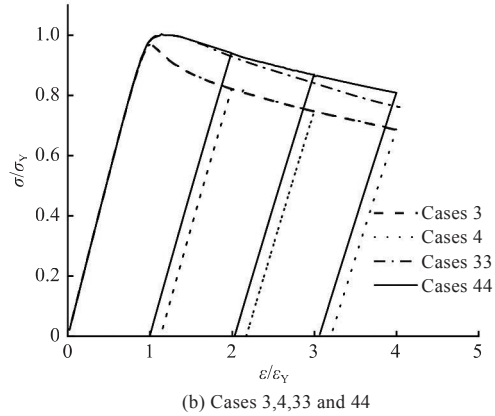

(b) Cases 3,4,33 and 44

Fig. 5 Average stress-strain curves

3.3 Von Mises stress distribution in limit state of stiffened plate under cyclic compressive-tensile loading

Figs. 6-8 illustrate contours of von Mises stress in each compressive limit state of the stiffened plate using ideal elastoplastic and cyclic plastic Chaboche material models separately under the same cyclic loading amplitude, in Cases 6 and 66. The red zones in these figures represent plastic yield zones. In Case 6, with the ideal elastoplastic material model, the plastic yield zone is widely distributed in the whole model in each limit state. However, with the cyclic plastic material model, in Case 66, the plastic yield zone in each limit state is locally concentrated and shrinks obviously with the increase in the number of cycles. This indicates that cyclic plasticity greatly affects the plastic yield of the stiffened plate under cyclic loading, which should be carefully considered in the analysis of ultimate strength.

3.4 Average stress-strain curves of stiffened plate under cyclic compressive-tensile loading

Fig. 9 shows average stress-strain curves in the case of using ideal elastoplastic and cyclic plastic Chaboche material models. The ultimate compressive and tensile strength of the stiffened plate under the Chaboche material model in the first cycle is higher than that under the ideal elastoplastic model.

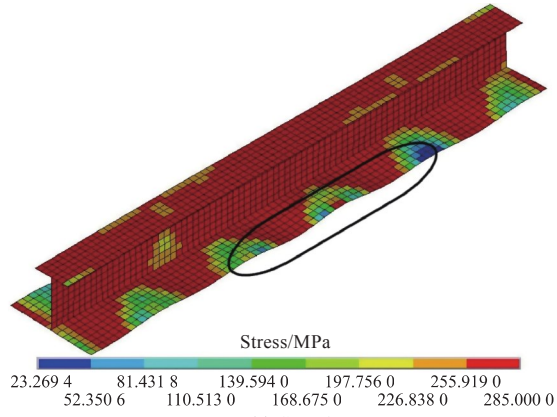

(a) Case 6

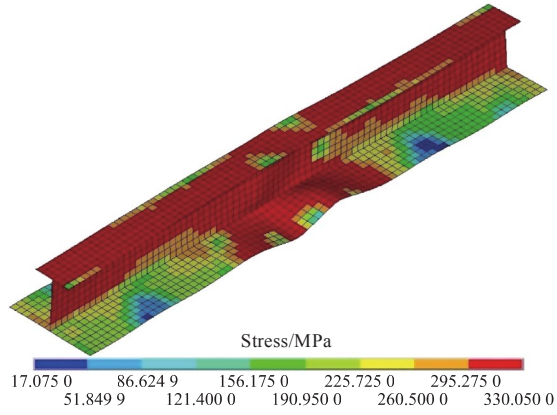

(b) Case 66

Fig. 6 First compressive limit state of Case 6 and Case 66

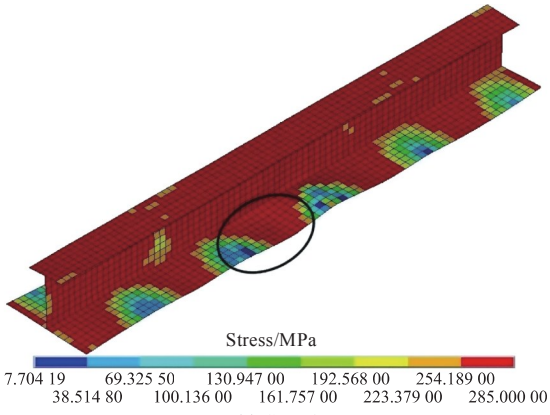

(a) Case 6

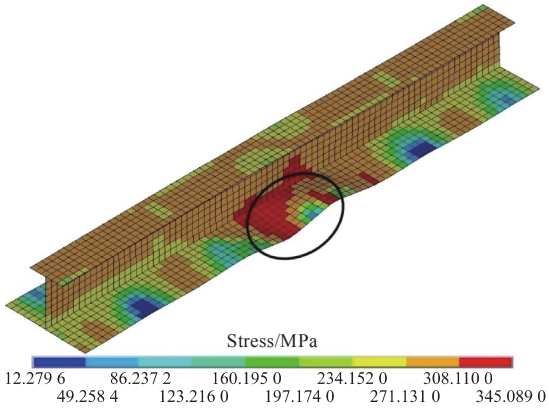

(b) Case 66

Fig. 7 Second compressive limit state of Case 6 and Case 66

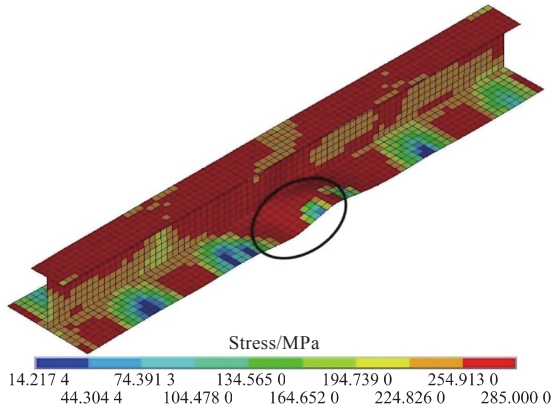

(a) Case 6

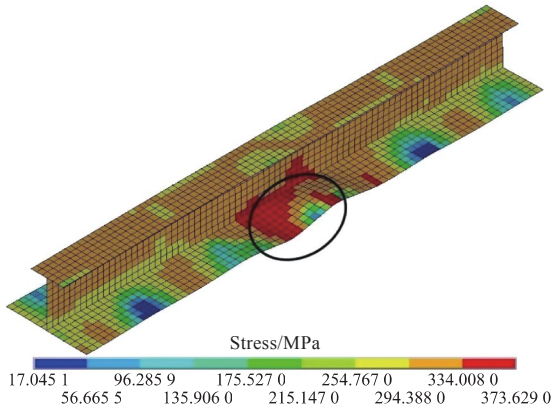

(b) Case 66

Fig. 8 Third compressive limit state of Case 6 and Case 66

In the subsequent cycles, the ultimate compressive strength under the ideal elastoplastic model obviously drops compared with that under the Chaboche material model. The ultimate tensile strength of the stiffened plate under the Chaboche material model is slightly higher than that under the ideal elastoplastic model in each cycle. Generally, the stiffened plate using the Chaboche material model shows a stable ultimate load-bearing behavior under cyclic compressive-tensile loading. Moreover, the plate undergoes a gentler reduction in ultimate compressive and tensile strength under the Chaboche material model than it does under the ideal elastoplastic model. Average stress-strain curves of 10 cycles shown in Fig. 10 also reflect similar characteristics.

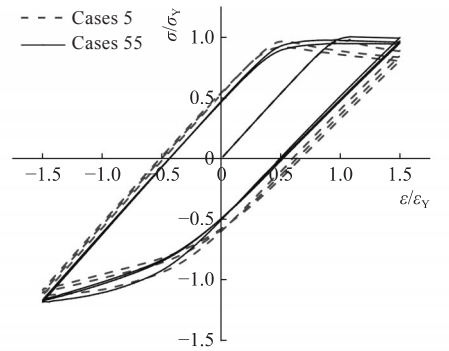

(a) Cases 5, 55

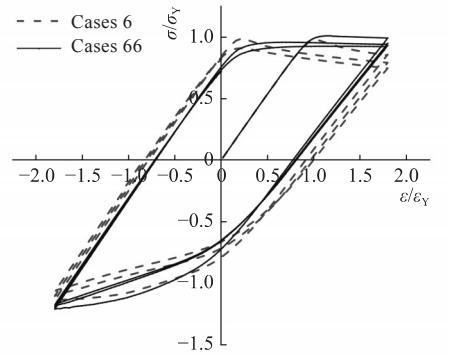

(b) Cases 6, 66

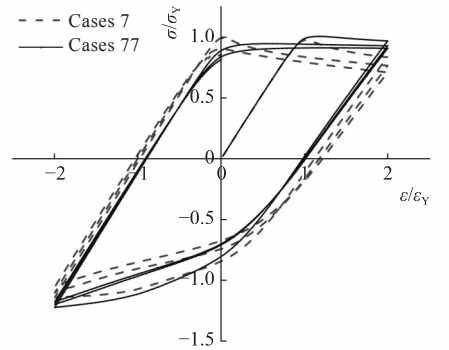

(c) Cases 7, 77

Fig. 9 Average stress-strain curves of stiffened plate under three cycles of loads

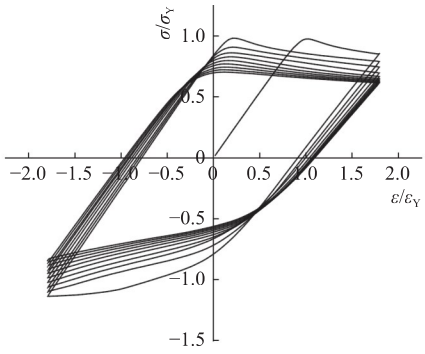

(a) Cases 8

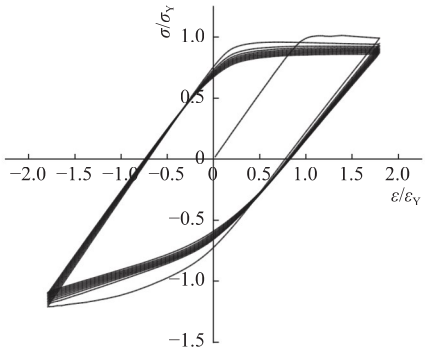

(a) Cases 88

Fig. 10 Average stress-strain curves of stiffened plate under ten cycles of loads

4 Conclusions

This paper comparatively analyzed the ultimate load-bearing behavior of stiffened plates of the same size with ideal elastoplastic, isotropic hardening, and cyclic plastic Chaboche material models under axial cyclic loading through nonlinear FE simulations. By analyzing the distribution of von Mises stress in the limit state of each cycle, the paper discusses the plastic yield distribution of a stiffened plate. Moreover, it studies the ultimate load-bearing behavior of the stiffened plate under different material models according to average stress-strain curves. The main conclusions obtained are as follows:

1) Under cyclic compressive loading or cyclic compressive-tensile loading, the plastic yield zone of the ideal elastoplastic material model is most widely distributed in the compressive limit state.

2) With the addition of cyclic plasticity, the plastic yield zone of the stiffened plate in each compressive limit state is gradually concentrated locally and tends to shrink gradually.

3) The ultimate compressive strength of the isotropic hardening material model in various cycles is always higher than that of the ideal elastoplastic material model. The ultimate compressive strength of both material models in various cycles always decreases with the increase in strain.

4) The introduction of the cyclic plastic material model makes the stiffened plate have more stab ultimate load-bearing behavior under cyclic loading than it does with the ideal elastoplastic material model.

References

[1] CALDWELL J B. Ultimate longitudinal strength [J]. Transactions of RINA, 1965, 107: 411−430.

[2] IACS. Common structural rules for double hull oil tankers [S]. London: International Association of Classification Societies, 2006.

[3] IACS. Common structural rules for bulk carriers [S]. London: International Association of Classification Societies, 2006.

[4] ISO. Ships and marine technology-ship structures-Part 1: general requirements for their limit state assessment: ISO 18072-1 [S]. Geneva, Switzerland: ISO, 2007.

[5] IMO. Goal-based standards [S]. London, UK: International Maritime Organization, 2010.

[6] IMO. Harmonised common structural rules (HCSR) for oil tankers and bulk carriers: MSC 87/5/6 [S]. London, UK: International Association of Classification Societies (IACS), 2012.

[7] MURRAY J M. Structural development of tankers [J]. European shipbuilding, 1953, 3(5).

[8] EVANS J H. Concept of ship structure design [M]. SANG G G, CHEN S K, WANG X F, et al, trans. Beijing:National Defense Industry Press, 1985 (in Chinese).

[9] FUJITA Y, NOMOTO T, YUGE K. Behavior of deformation of structural members under compressive and tensile loads (18 report)—on the buckling of a column subjected to repeated loading [J]. Journal of the Society of Naval Architects of Japan, 1984, 156: 346−354.

[10] HUANG Z Q. A new view on the criterion of total hull strength for sea-going ships [J]. Wuhan Shipbuilding, 1993 (6): 8−12 (in Chinese).

[11] HUANG Z Q, CHEN Q S, LUO Z Y. Ultimate longitudinal strength of ship's hull girder under cyclic bending loads [J]. Shipbuilding of China, 1996 (3): 87−95 (in Chinese).

[12] HUANG Z Q. Some problems in the study of ship's strength [J]. Wuhan Shipbuilding, 1999 (3): 1−5 (in Chinese).

[13] CUI H W, YANG P. Ultimate strength assessment of hull girder under cyclic bending based on smith's method [J]. Journal of Ship Research, 2018, 62 (2): 77−88.

[14] CUI H W, YANG P. Ultimate strength of hull plates under monotonic and cyclic uniaxial compression [J]. Journal of Ship Research, 2018, 62 (3): 156−165.

[15] CUI H W, YANG P. Ultimate strength and failure characteristics research on steel box girders under cyclic bending moments [J]. Journal of Marine Science and Technology, 2018, 23(4): 926−936.

[16] CUI H W, YANG P. Cyclic behavior of stiffened plates

under in-plane loading by numerical analysis [C] // Proceedings of the ASME 2014 33rd International Conference on Ocean, Offshore and Arctic Engineering. San Francisco, California, USA: ASME, 2014.

[17] CUI H W, YANG P, CUI C. Experimental research on ultimate strength of plates under cyclic axial loads [C] // Proceedings of the Twenty-fifth International Ocean and Polar Engineering Conference. Kona, Big Island, Hawaii, USA: ISOPE, 2015.

[18] JONES N. On the shakedown limit of a ship's hull girder[J]. Journal of Ship Research, 1975, 19(2): 118−121.

[19] GANNON L G, PEGG N G, SMITH M J, et al. Effect of residual stress shakedown on stiffened plate strength and behaviour [J]. Ships and Offshore Structures, 2013, 8 (6): 638−652.

[20] ZHANG X M, PAIK J K, JONES N. A new method for assessing the shakedown limit state associated with the breakage of a ship's hull girder [J]. Ships and Offshore Structures, 2016, 11 (1): 92−104.

[21] SMITH C S. Influence of local compressive failure on ultimate longitudinal strength of a ship's hull [C] // Proceedings of the International Symposium on PRADS. Tokyo, Japan: [s. n.], 1977: 73−79.

[22] HUGHES O F, PAIK J K. Ship structural analysis and design [M]. [s. l.]: Society of Naval Architects and Marine Engineers, 2010.

[23] LI S, HU Z Q, BENSON S. An analytical method to predict the buckling and collapse behaviour of plates and stiffened panels under cyclic loading [J]. Engineering Structures, 2019, 199: 109627.

[24] LEMAITRE J, CHABOCHE J L. Mechanics of solid materials [M]. Cambridge, UK: Cambridge University Press, 1990.

[25] KROLO P, GRANDIĆD, SMOLČIĆŽ. Experimental and numerical study of mild steel behaviour under cyclic loading with variable strain ranges [J]. Advances in Materials Science and Engineering, 2016, 2016: 7863010.

轴向循环载荷下加筋板极限承载性能分析

崔虎威*, 丁启印

重庆交通大学 航运与船舶工程学院, 重庆 400074

摘　要: [**目的**] 为提高船体加筋板极限承载性能非线性数值模拟的准确性, 研究理想弹塑性、各向同性强化及循环塑性Chaboche材料模型对加筋板极限状态时的塑性屈服分布及压缩、拉伸极限强度的影响。[**方法**] 针对某同一尺寸加筋板, 采用ANSYS软件开展轴向循环压缩、循环压缩—拉伸载荷下的极限承载性能非线性有限元数值模拟。[**结果**] 结果显示, 不同的材料属性对加筋板极限承载性能及极限状态时的塑性屈服分布具有显著影响; 在开展船体加筋板极限承载性能非线性有限元数值模拟时, 需要根据不同的载荷形式选择恰当的材料模型。[**结论**] 所得结果对进一步研究船体结构在循环载荷作用下的极限强度特性及累积塑性破坏机理具有一定的参考价值。

关键词: 循环载荷; 加筋板; 循环塑性; 极限强度